Examination of how properties of a fissioning system impact isomeric yield ratios of the fragments

D. Gjestvang,[1,*] J. N. Wilson,[2] A. Al-Adili,[3] S. Siem,[1] Z. Gao,[3] J. Randrup,[4] D. Thisse,[2] M. Lebois,[2] N. Jovančević,[5] R. Canavan,[6,7] M. Rudigier,[6,8] D. Étasse,[9] R.-B. Gerst,[10] E. Adamska,[11] P. Adsley,[2] A. Algora,[12,13] C. Belvedere,[6] J. Benito,[14,15] G. Benzoni,[16] A. Blazhev,[10] A. Boso,[7] S. Bottoni,[16,17] M. Bunce,[7] R. Chakma,[2] N. Cieplicka-Oryńczak,[18] S. Courtin,[19] M. L. Cortés,[20] P. Davies,[21] C. Delafosse,[2] M. Fallot,[22] B. Fornal,[18] L. Fraile,[14] A. Gottardo,[23] V. Guadilla,[22] G. Häfner,[2,10] K. Hauschild,[2] M. Heine,[19] C. Henrich,[8] I. Homm,[8] F. Ibrahim,[2] Ł. W. Iskra,[16,18] P. Ivanov,[7] S. Jazrawi,[6,7] A. Korgul,[11] P. Koseoglou,[8,24] T. Kröll,[8] T. Kurtukian-Nieto,[25] S. Leoni,[16,17] J. Ljungvall,[2] A. Lopez-Martens,[2] R. Lozeva,[2] I. Matea,[2] K. Miernik,[11] J. Nemer,[2] S. Oberstedt,[26] W. Paulsen,[1] M. Piersa-Siłkowska,[11] Y. Popovitch,[2] C. Porzio,[16,17,27,†] L. Qi,[2] P. H. Regan,[6,7] K. Rezynkina,[28] V. Sánchez-Tembleque,[14] C. Schmitt,[19] P.-A. Söderström,[8,29] C. Sürder,[8] G. Tocabens,[2] V. Vedia,[14] D. Verney,[2] N. Warr,[10] B. Wasilewska,[18] J. Wiederhold,[8] M. Yavahchova,[30] and S. Ziliani[16,17]

[1]*Department of Physics, University of Oslo, N-0316 Oslo, Norway*
[2]*Université Paris-Saclay, CNRS/IN2P3, IJC Laboratory, Orsay, France*
[3]*Department of Physics and Astronomy, Uppsala University, Uppsala 75120, Sweden*
[4]*Nuclear Science Division, Lawrence Berkeley National Laboratory, Berkeley, California 94720, USA*
[5]*Faculty of Sciences, University of Novi Sad, Novi Sad, Serbia*
[6]*Department of Physics, University of Surrey, Guildford, United Kingdom*
[7]*National Physical Laboratory, Teddington, United Kingdom*
[8]*Institut für Kernphysik, Fachbereich Physik, Technische Universität Darmstadt, Darmstadt, Germany*
[9]*LPC Caen, Caen, France*
[10]*Institut für Kernphysik, Universität zu Köln, Cologne, Germany*
[11]*Faculty of Physics, University of Warsaw, Warsaw, Poland*
[12]*IFIC, CSIC–University of Valencia, Valencia, Spain*
[13]*Institute for Nuclear Research (Atomki), Debrecen, Hungary*
[14]*Grupo de Fisica Nuclear & IPARCOS, Universidad Complutense de Madrid, CEI Moncloa, Madrid, Spain*
[15]*Dipartimento di Fisica dell'Università, and Istituto Nazionale di Fisica Nucleare, Sezione di Padova, I-35131 Padova, Italy*
[16]*INFN Sezione Milano, Milandelo, Italy*
[17]*Dipartimento di Fisica, Universitá degli Studi di Milano, Milan, Italy*
[18]*Institute of Nuclear Physics, Polish Academy of Sciences, Krakow, Poland*
[19]*Université de Strasbourg, CNRS, IPHC UMR 7178, Strasbourg, France*
[20]*RIKEN Nishina Center, Hirosawa, Japan*
[21]*School of Physics and Astronomy, University of Manchester, Manchester, United Kingdom*
[22]*Subatech, IMT-Atlantique, Université de Nantes, Nantes, France*
[23]*INFN Laboratori Nazionali di Legnaro, Legnaro, Italy*
[24]*GSI Helmoltzzentrum für Schwerionenforschung GmbH, Darmstadt, Germany*
[25]*Université de Bordeaux, CNRS, CENBG UMR 5797, Gradignan, France*
[26]*Joint Research Centre, European Commission, Geel, Belgium*
[27]*TRIUMF, Vancouver, British Columbia, Canada*
[28]*Institute for Nuclear and Radiation Physics, Katholieke Universiteit Leuven, Leuven, Belgium*
[29]*Extreme Light Infrastructure–Nuclear Physics, Horia Hulubei National Institute for Physics and Nuclear Engineering, Bucharest-Măgurele, Romania*
[30]*Institute for Nuclear Research and Nuclear Energy, Bulgarian Academy of Sciences, Sofia, Bulgaria*

(Received 31 March 2023; accepted 11 October 2023; published 4 December 2023)

The population of isomeric states in the prompt decay of fission fragments—so-called isomeric yield ratios (IYRs)—is known to be sensitive to the angular momentum J that the fragment emerged with, and may therefore contain valuable information on the mechanism behind the fission process. In this work, we investigate how changes in the fissioning system impact the measured IYRs of fission fragments to learn more about what parameters affect angular momentum generation. To enable this, a new technique for measuring IYRs is first demonstrated. It is based on the time of arrival of discrete γ rays, and has the advantage that it enables the study of the IYR as a function of properties of the partner nucleus. This technique is used to extract the IYR of ^{134}Te,

*dorthea.gjestvang@fys.uio.no
†Current address: Nuclear Science Division, Lawrence Berkeley National Laboratory, Berkeley, CA 94720, USA.

strongly populated in actinide fission, from the three different fissioning systems: ^{232}Th(n, f), ^{238}U(n, f), at two different neutron energies, as well as ^{252}Cf(sf). The impacts of changing the fissioning system, the compound nuclear excitation energy, the minimum J of the binary partner, and the number of neutrons emitted on the IYR of ^{134}Te are determined. The decay code TALYS is used in combination with the fission simulation code FREYA to calculate the primary fragment angular momentum from the IYR. We find that the IYR of ^{134}Te has a slope of 0.004 ± 0.002 with increase in compound nucleus (CN) mass. When investigating the impact on the IYR of increased CN excitation energy, we find no change with an energy increase similar to the difference between thermal and fast fission. By varying the mass of the partner fragment emerging with ^{134}Te, it is revealed that the IYR of ^{134}Te is independent of the total amount of prompt neutrons emitted from the fragment pair. This indicates that neutrons carry minimal angular momentum away from the fission fragments. Comparisons with the FREYA+TALYS simulations reveal that the average angular momentum in ^{134}Te following ^{238}U(n, f) is $6.0\hbar$. This is not consistent with the value deduced from recent CGMF calculations. Finally, the IYR sensitivity to the angular momentum of the primary fragment is discussed. These results are not only important to help understanding the underlying mechanism in nuclear fission, but can also be used to constrain and benchmark fission models, and are relevant to the γ-ray heating problem of reactors.

DOI: 10.1103/PhysRevC.108.064602

I. INTRODUCTION

An intriguing aspect of the nuclear fission process is the generation of angular momenta in the fission fragments, which occurs even when the fissioning nucleus starts with no net angular momentum [1]. New experimental results have emerged and revealed more details on the nature of this process [2–4], and both theoretical and experimental efforts are being made to uncover further aspects of the mechanism behind it [5–7].

One of the challenges related to the study of angular momentum generation is that the angular momentum magnitude of the primary fragment J_i is not directly measurable. Therefore, experimental investigations are restricted to quantities that are merely sensitive to J_i. In those fragments that have long-lived isomeric states, such a quantity is the isomeric yield ratio (IYR) of the fragment [8], defined as the relative frequency at which the fragment is populated in the isomeric state of a given spin. The IYR is known to be sensitive to changes in the angular momentum of the fragment [9], and comparing measured IYRs from different fissioning systems and configurations thus gives insight into what impacts the generation of angular momentum in fission fragments.

In addition to the basic science interest, measurements of isomeric yield ratios are also relevant for other related nuclear energy and fundamental applications such as the determination of the decay heat in reactors and the determination of the antineutrino spectrum from reactors. The isomeric yield ratio impacts the population of β decaying isomers [10], that can have different contributions to both decay heat and antineutrino spectrum (see for example Ref. [11] in relation to the summation method [12]).

It has also been pointed out that one of the main challenges with predicting γ-ray heating of reactors is that the excitation energy and angular momentum distributions among fission fragments are not well known [13]. Here, IYR measurements serve as benchmarks for fission models and thus contribute to more accurate reactor simulations.

Isomeric yield ratios of fission fragments have been studied since the 1950s [14,15], and measurement methods include radiochemical separation [16,17], in-flight mass spectrometry [18], both followed by γ-ray counting, as well as direct ion counting in a Penning trap [19]. There are advantages and drawbacks with each method, and they are also sensitive to different isomeric lifetime ranges.

In this paper we present a new method for extracting isomeric yield ratios. This method can reach isomer half-lives on the order of 10^{-8}–10^{-6}s without the need for knowing the γ-feeding intensities between levels or correcting for unobserved isomer decay.

Using this technique, we study IYR variation with mass and energy of the fissioning system and introduce the procedure of partner gating, where demands are put on the mass, charge and minimum angular momentum of the binary fragment partner. By looking for small relative changes in the measured IYR, we gain an understanding of how changes in these properties affect the IYR—and therefore angular momentum—of fission fragments.

In this work we focus on the 6^+ isomeric state in the ^{134}Te fission fragment, for which the IYRs are measured for the first time. This fragment was chosen because it is strongly populated in the fission of actinides, the 164.1 ± 0.9 ns isomer half-life [20] is suitable with respect to the beam pulsation, and the emitted γ rays from the subsequent cascade can be efficiently detected.

We also combine the fission simulation code FREYA [21] with the nuclear reaction code TALYS to reproduce the measured IYR, which allows us to transform from the IYR to the initial distribution of angular momentum that ^{134}Te emerged with. This procedure has previously been demonstrated using the GEF fission code [22]. Finally, the sensitivity of IYRs on the initial angular momentum in the fission fragment is discussed.

II. EXPERIMENTAL DETAILS

The data presented in this paper was collected during the ν-Ball fission campaign at the ALTO facility of IJC Laboratory, Orsay [23]. The ν-Ball spectrometer is a hybrid array, at

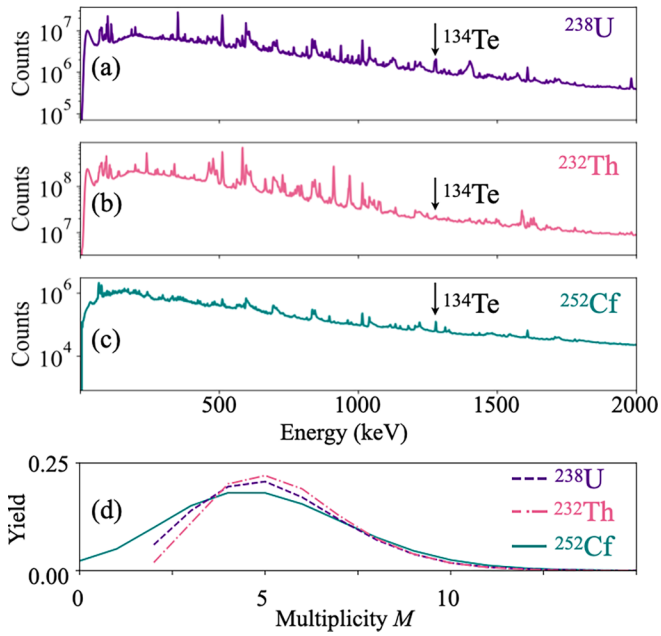

FIG. 1. The experimental E_γ spectrum for the reactions (a) ^{238}U(n, f) and (b) ^{232}Th(n, f) at $\bar{E}_n = 1.9$ and 2.0 MeV respectively; (c) ^{252}Cf(sf); as well as (d) the multiplicity distribution M for fission events. The 1279 keV γ ray from ^{134}Te is indicated in (a)–(c). In (d), the shape of the ^{238}U/^{232}Th multiplicity distributions are slightly different from ^{252}Cf due to the exclusion of $M < 2$ events, as described in the text. The distributions are therefore normalized in the range $M = [2, 15]$.

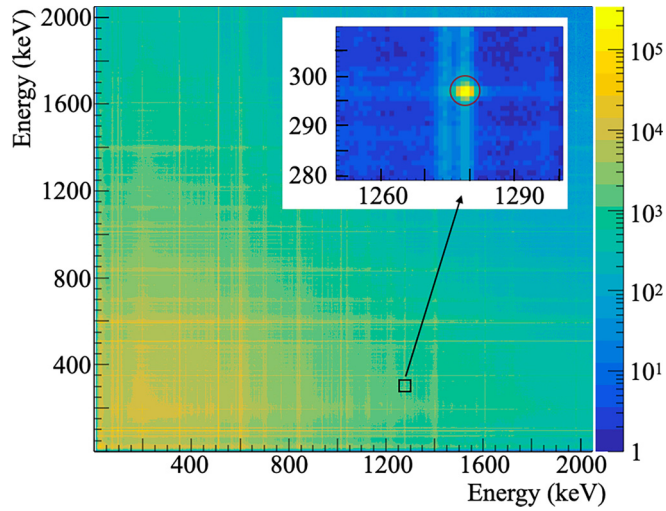

FIG. 2. The experimental $E_\gamma - E_\gamma$ coincidence spectrum following ^{238}U(n, f) at $\bar{E}_n = 1.9$ MeV. The circle in the inset shows coincidences between the 1279 and 297 keV γ rays following the decay of ^{134}Te.

the time consisting of 10 coaxial Compton-suppressed high-purity germanium (HPGe) detectors, 24 clover detectors, and 20 $LaBr_3$ detectors [24]. Only the Ge detectors were utilized for this analysis, and the overall Ge efficiency was around 5.5% at 1 MeV.

Three different fission reactions were used to populate ^{134}Te: the reactions ^{238}U(n, f) and ^{232}Th(n, f) induced with fast neutrons, and spontaneous fission of ^{252}Cf. An ionization chamber was placed in the middle of ν-Ball for the ^{252}Cf measurements, and the detection of a fission fragment in the cathode was used to trigger the data acquisition. For more details, see Ref. [25].

The neutron-induced fission experiments were achieved by coupling ν-Ball to the LICORNE neutron source, which produces a directional beam of neutrons using the inverse-kinematics reaction $p(^7\mathrm{Li}, n)\,^7\mathrm{Be}$ [26]. Neutrons were delivered in 2-ns-wide pulses every 400 ns. The average neutron energy $\bar{E}_n$ that induced fission was 1.9 MeV for ^{238}U(n, f) and 2.0 MeV for ^{232}Th(n, f), both with a dispersion of 0.4 MeV. Additionally, a data set was collected for ^{238}U(n, f) with $\bar{E}_n = 3.4$ MeV and a dispersion of 0.3 MeV. The values of $\bar{E}_n$ correspond to ^{239}U fissioning with an average excitation energy of $\bar{E}_\mathrm{x} = 6.7$ and 8.2 MeV respectively, while $\bar{E}_\mathrm{x}$ was 6.8 MeV for ^{233}Th. From the dispersion we see that the values for the high and low $\bar{E}_\mathrm{x}$ for ^{238}U(n, f) are significantly different.

All data were written to file using the FASTER digitalization system [27] and processed later offline. In the neutron-induced fission experiments both fragments were immediately stopped in the thick target, whereas in the case of ^{252}Cf one fragment was detected in flight.

The analysis was conducted differently for the cases of ^{252}Cf versus ^{238}U and ^{232}Th. In the ^{252}Cf case, the ionization chamber gave a clear tag on fission events, resulting in a compact data set with minimal background from other reactions. In this case, Compton-suppressed γ rays within a 4 μs time window were written to file for further analysis.

In the case of the neutron-induced fission experiments, both fragments were stopped in the target. The selection of fission events, e.g., the fission trigger, was based on the total number of γ rays detected in a given beam burst, referred to as the multiplicity M of the event. Due to the large number of γ rays emitted in fission compared to background reactions of, e.g., neutron scattering, higher-M events are increasingly dominated by fission. To first order, events with $M \geqslant 2$ were selected. By further testing the multiplicity condition we found that $M \geqslant 4$ was the optimal requirement that did not impact the extracted IYRs while at the same time minimizing the background and retaining the majority of the fission events. The resulting γ-ray spectra measured for the three different reactions as well as the M distributions can be seen in Fig. 1.

The γ rays detected in the same event were thereafter sorted into a cube with $E_\gamma - E_\gamma - T$ for the analysis, where T is the arrival time of the highest-energy γ ray relative to the beam burst. The $E_\gamma - E_\gamma$ spectrum following ^{238}U(n, f) for any T is shown in Fig. 2.

III. METHOD

We present here the new technique for extracting isomeric yield of fission fragments and demonstrate it on the particular case of ^{134}Te. The level scheme of the lowest excited states in ^{134}Te is illustrated in Fig. 3, where the isomeric state is indicated.

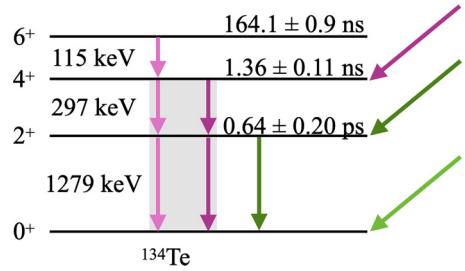

FIG. 3. Illustration of the lowest-lying levels of ^{134}Te, constructed using energies and feeding values found in Ref. [20]. There are no additional transitions between the levels, i.e., the 6^+ state decays only to the 4^+ state, etc. The side-feeding branches, where the decay bypasses, e.g., the 4^+ and goes directly to the 2^+, are also indicated. The shaded area represents the double gate on discrete γ rays used in this work.

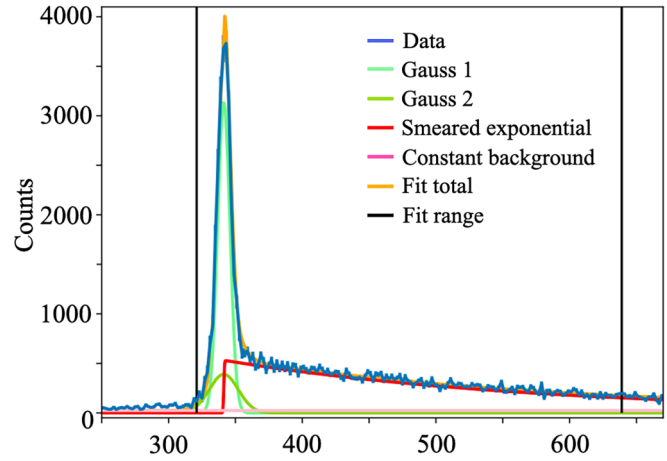

FIG. 4. Background-subtracted spectrum showing the time of arrival of a pair of 297 and 1279 keV γ rays, created using gates on the $4^+ \rightarrow 2^+$ and $2^+ \rightarrow 0^+$ transitions in ^{134}Te. The components of the fitted spectrum are also shown, along with the fit range.

The method relies on detecting the time of arrival of discrete γ rays. Ge detectors were used to gate on events where a pair of γ rays originating from states below the isomer were observed in coincidence. For ^{134}Te the selected γ rays are 297 and 1279 keV, and Fig. 3 illustrates how these come from the transitions $4^+ \rightarrow 2^+$ and $2^+ \rightarrow 0^+$ respectively. A pair of γ rays was chosen rather than a single one to minimize background, and the coincidence peak is shown in the inset of Fig. 3. Due to the need to observe discrete γ rays that are not Doppler broadened, the method is sensitive to γ rays emitted when the ^{134}Te fragment is stopped in either the target or the walls of the target chamber.

The γ rays of interest were selected by placing 5 keV wide energy gates around the peaks in the $\gamma - \gamma$ matrix. A background gate was put on either side of the true peak, and counts were subtracted if one or both of the two γ rays were in the background gate.

Using the time stamp from the highest-energy γ ray, a background-subtracted time-of-arrival spectrum was created. This spectrum is shown in Fig. 4 for the case of ^{238}U(n, f) with $\bar{E}_n = 1.9$ MeV.

After ^{134}Te was populated in fission, the de-excitation process could take different paths and either populate the isomer or bypass it. In the case when the isomer was bypassed, the pair of 297 and 1279 keV γ rays was observed to arrive promptly after fission. The shape of this prompt peak is best described by a sum of two Gaussians with the same mean, but different widths. On the other hand, if ^{134}Te was populated in the isomeric state, the arrival of the 297 and 1279 keV pair was observed delayed with respect to fission. The shape of this component is an exponential decay curve with the half-life characterized by the isomeric half-life of 164.1 ± 0.9 ns [20]. Finally, ^{134}Te might have been populated through β decay, in which the 297 and 1279 keV pair arrived uncorrelated from a prompt peak and gave rise to constant background. The combination of these three contributions describes the shape of the observed time spectrum in Fig. 4.

If the decay did not follow the yrast line and instead directly fed the 2^+ or 0^+ states in Fig. 3, then the 297 and 1279 keV pair would not be detected. These events are therefore not included in the spectrum of Fig. 4, and the impact of this on the determined IYR is discussed further in Sec. III B.

To determine the IYR, the prompt two-Gaussian and the delayed exponential contributions to the spectrum in Fig. 4 had to be decoupled. This was done using nonlinear least squares fitting, where the spectrum was described as a sum of two Gaussian curves, a delayed exponential decay curve, and a constant background, where the contributions are convoluted and smeared according to the time resolution of the prompt Gaussian. There were thus seven physics-based fitting parameters: the mean μ of the Gaussians, which also was the starting point for the exponential decay, the two widths of the Gaussians σ_1 and σ_2, the heights of both the Gaussians' peak and the exponential decay curve, and the level of constant background of β decay. The half-life of the isomeric state was fixed to the adopted literature value of 164.1 ns [20]. The total fits and its components are shown in Fig 4.

In the level scheme of ^{134}Te there is also a 18 ns 12^+ isomeric state [20], which feeds the 6^+ isomeric state. This state is very weakly populated in fission (<5%), and the only potential impact of this state would be a slight change of the rise-time slope of the delayed component in Fig. 4. As this change would have no significant impact on the measured IYR, it is therefore not considered.

Assuming both fission fragments are stopped promptly after fission, the IYR is then the area under the delayed exponential curve (integrated to "infinity," i.e., ≈70 half-lives) divided by the total area under the prompt two-Gaussian + delayed exponential:

$$\mathrm{IYR} = \frac{\text{delayed}}{\text{prompt} + \text{delayed}}. \quad (1)$$

In the case of ^{252}Cf, one of the fragments deexcited in flight. If the isomeric state was bypassed, the 297 and 1279 keV γ rays would therefore be Doppler broadened and not be included in the energy gate. Hence only half of the prompt peak was visible in the time spectrum, and the formula for the

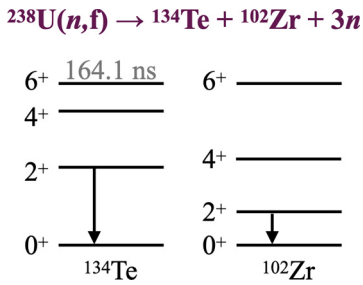

FIG. 5. Illustration of partner gating following ^{238}U(n, f), where one γ gate is placed in ^{134}Te and the other in ^{102}Zr.

IYR has an additional factor 2. The IYR is calculated using

$$\mathrm{IYR} = \frac{\text{delayed}}{2 \times \text{prompt} + \text{delayed}}. \quad (2)$$

The in-flight isomer decay is minimal and can be neglected.

Due to the timing properties of the ionization chamber, the prompt peak in the case of ^{252}Cf was found to be asymmetric. This was investigated by creating a double-gated time spectrum in a nucleus known to have no isomeric state, for example ^{140}Xe. Based on this, a smeared exponential tail was included in the fit of the prompt peak.

A. Uncertainties

The uncertainties on the calculated IYRs were determined by a Monte Carlo resampling method. First, the statistical uncertainty on each bin in the spectrum of Fig. 4 was calculated based on the amounts of counts in the unsubtracted and background spectra. The spectrum was then resampled, where each data bin was varied according to the statistical uncertainty of that bin. The resulting fit was thus slightly perturbed, giving a different value of the calculated IYR. This procedure was repeated $N = 5000$ times, and the variation in the calculated IYRs revealed the uncertainty on the measurement. N was chosen to be sufficiently high such that the value of the uncertainty converged. In addition to the statistical uncertainty, we included a 5% systematic variation in the background as well as a variation in the fit range of the spectrum.

B. Partner gating

In the previous sections it was described how γ gating is used to obtain the IYR of ^{134}Te, and the procedure was illustrated by using gates on the lowest $4^+ \rightarrow 2^+$ and $2^+ \rightarrow 0^+$ transitions in ^{134}Te. The notation $2^+[^{134}\mathrm{Te}]\&4^+[^{134}\mathrm{Te}]$ will be used to indicate this γ gating.

A new aspect of this method is that when both fragments are stopped in the target, gates can be placed on a specific partner that emerges with the ^{134}Te. For example, in ^{238}U(n, f), ^{134}Te can emerge in the system:

$$^{238}\mathrm{U}(n, \mathrm{f}) \rightarrow {}^{134}\mathrm{Te} + {}^{102}\mathrm{Zr} + 3n. \quad (3)$$

By gating on the transitions $2^+ \rightarrow 0^+$ in ^{134}Te as well as $2^+ \rightarrow 0^+$ in ^{102}Zr as illustrated in Fig. 5, events are selected where the prompt neutron multiplicity was 3. If the second gate is instead put in ^{100}Zr or ^{104}Zr, the IYR can be extracted in the cases when ^{134}Te arrived with $5n$ or $1n$ respectively. This partner gating technique effectively enables the study of the sensitivity of the IYR (and thus J_i) to the prompt neutron multiplicity. This gives insight into how much angular momentum the neutrons remove from the initial fission fragment and is highly relevant, as the paradigm that they carry only negligible amounts has recently been brought into question [28].

We note here that the partner gating technique will not give the same values for the IYR as the double gate on $2^+[^{134}\mathrm{Te}]\&4^+[^{134}\mathrm{Te}]$. In the double gate, the events where the decay bypass the 4^+ and directly populate the 2^+ were excluded in the calculated IYR. In the partner gate of Fig. 5, where only a gate on $2^+[^{134}\mathrm{Te}]$ is used, the 2^+ side-feeding branch was included. Since all the direct feeding to the 2^+ state bypassed the isomer, this resulted in a lower value for the IYR. The choice of gating thus changes the value of the IYR. This is unproblematic: we are interested in a relative comparison between systems where the same gating is used to study the impact on the IYR, as the IYR value in itself says little about the system. Furthermore, any technique that relies on the detection of γ rays will also omit the direct feeding to the ground state, so the impact of gating is already present in previous measurements. Finally, extracted IYRs can be used to either constrain or benchmark fission fragment decay simulations, as will be demonstrated in Sec. V. This can be done no matter which gates were used to extract the IYR.

Time spectra like the one in Fig. 4 are slightly different for the partner gate compared to the double gate. As ^{134}Te only emerge in coincidence with a partner nucleus in the case of fission, there is no constant background of β decay observed in these spectra. The constant-background parameter in the fit is therefore fixed to zero.

Another possibility opened up with the partner gating technique is to select increasing amounts of angular momenta in the partner nucleus. In Fig. 5, gates were placed on the transition $2^+ \rightarrow 0^+$ in ^{102}Zr; however, one may instead put this gate higher up in the level scheme, on $4^+ \rightarrow 2^+$ or $6^+ \rightarrow 4^+$, and so on. As the minimum angular momentum of ^{102}Zr is increased and the IYR of ^{134}Te is extracted in each case, potential correlations in the magnitudes of the two angular momenta of the fragments are investigated. The degree of correlation between the magnitudes of the two angular momenta gives insight into the angular momentum generation process, and obtaining more data on this would therefore be valuable.

C. Advantages

One advantage of the new method presented is that there is no need to correct the calculated IYR for radioactive decay. For some methods there is a significant amount of time between the moment of fission and the measurement, such that the isomer might have time to decay before detection [19]. Ours is a prompt measurement and does not have this drawback.

Furthermore, other methods are unable to determine directly whether the isomer was populated by prompt decay of fission fragments or after β decay. Since β decay will populate a different spin distribution compared to fission,

TABLE I. Isomeric yield ratio of ^{134}Te extracted from the reactions ^{238}U(n, f), ^{232}Th(n, f), and ^{252}Cf(sf), with the employed gates indicated.

Reaction	$\bar{E}_n$ (MeV)	Gate type	Gate transitions	Gate energies (keV)	IYR
^{238}U(n, f)	1.9	double gate	2^+[^{134}Te] & 4^+[^{134}Te]	1279 & 297	0.73 ± 0.01
		1n	2^+[^{134}Te] & 4^+[^{104}Zr]	1279 & 312	0.65 ± 0.05
		3n	2^+[^{134}Te] & 4^+[^{102}Zr]	1279 & 326	0.69 ± 0.02
		3n-partner 2^+	2^+[^{134}Te] & 2^+[^{102}Zr]	1279 & 151	0.61 ± 0.06
		3n-partner 4^+	2^+[^{134}Te] & 4^+[^{102}Zr]	1279 & 326	0.69 ± 0.02
		3n-partner 6^+	2^+[^{134}Te] & 6^+[^{102}Zr]	1279 & 487	0.67 ± 0.03
^{238}U(n, f)	3.4	double gate	2^+[^{134}Te] & 4^+[^{134}Te]	1279 & 297	0.74 ± 0.04
^{232}Th(n, f)	2.0	double gate	2^+[^{134}Te] & 4^+[^{134}Te]	1279 & 297	0.68 ± 0.03
		1n	2^+[^{134}Te] & 6^+[^{98}Sr]	1279 & 433	0.6 ± 0.1
		3n	2^+[^{134}Te] & 2^+[^{96}Sr]	1279 & 815	0.62 ± 0.03
		4n	2^+[^{134}Te] & $\frac{3}{2}^+$[^{95}Sr]	1279 & 352	0.6 ± 0.1
		3n-partner 2^+	2^+[^{134}Te] & 2^+[^{96}Sr]	1279 & 815	0.62 ± 0.03
		3n-partner 4^+	2^+[^{134}Te] & 4^+[^{96}Sr]	1279 & 978	0.47 ± 0.03
^{252}Cf(sf)	N/A	double gate	2^+[^{134}Te] & 4^+[^{134}Te]	1279 & 297	0.77 ± 0.02

contamination from β-decay feeding will impact the measured IYR. Only the prompt IYR reflects the initial fragment angular momentum J_i, and hence uncontaminated IYR measurements are needed for investigating angular momentum effects in fission. The β-decay feeding must thus be either minimal due to a long precursor lifetime or corrected for, which will introduce additional uncertainties in the extracted IYR.

The fission tag in the case of ^{252}Cf and the $M \geqslant 4$ multiplicity condition for ^{232}Th and ^{238}U renders the β-decay background small (e.g., for Fig. 4, the constant background is 5% of the counts within the fit region). Additionally, the β-decay feeding manifests itself as a constant background in the time spectrum (pink line in Fig. 4) and is therefore easily subtracted. Furthermore, the partner-gated spectra do not have a background of β decay, as explained above. We are thus able to measure the IYR without the contamination from β-decay isomer feeding.

Finally, this method does not rely on previously measured γ-ray feeding intensities nor on the experimentally determined efficiency of the detector array. Both of these have been identified as potential sources of systematic uncertainties of IYR measurements [29].

The unique feature of partner gating enables the study of the sensitivity to changes in a fragment's J_i with partner nucleus spin or neutron multiplicity.

Another advantage, not with the method but with this data set, is that all three different fissioning systems were measured in the same experimental campaign and using the same detector array. This analysis thus also avoids systematic differences between measurements that could potentially give rise to artificial variations in the IYRs. Hence, we can be more confident that potential deviations between IYRs across the different systems actually reflect underlying physics.

Finally, the present technique as well as IYR measurements in general are complementary to the J_i-sensitive measurement method developed by the University of Manchester [30]. Though IYR measurements are limited to fission fragments with suitable isomers, they might be sensitive to small changes in the J_i distribution.

IV. RESULTS

The IYR of ^{134}Te was extracted following the reactions ^{238}U(n, f) and ^{232}Th(n, f) induced with fast neutrons [$\bar{E}_n$ = 1.9 and 3.3 MeV for ^{238}U(n, f) and 2.0 MeV for ^{232}Th(n, f)], and spontaneous fission of ^{252}Cf. In the case of neutron-induced fission, partner gating was employed to extract the IYRs for various numbers of emitted neutrons emitted as well as minimum spin of the partner. The results are summarized in Table I and illustrated in Figs. 6–8. The difference in IYR between a double gate in ^{134}Te and a partner gate is expected as commented in Sec. III B and is due to the omission of the 2^+ side feeding branch when using a double gate.

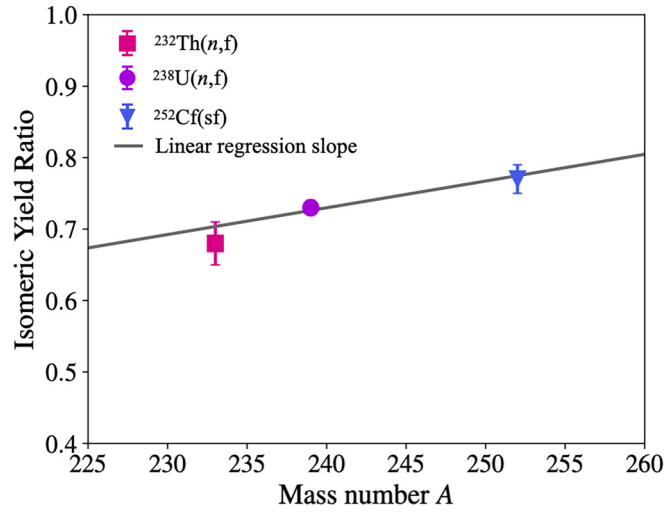

FIG. 6. Isomeric yield ratios of ^{134}Te as a function of the compound nucleus mass number, using gates on 2^+[^{134}Te]&4^+[^{134}Te]. The linear uncertainty-weighted fit to the data points is also shown.

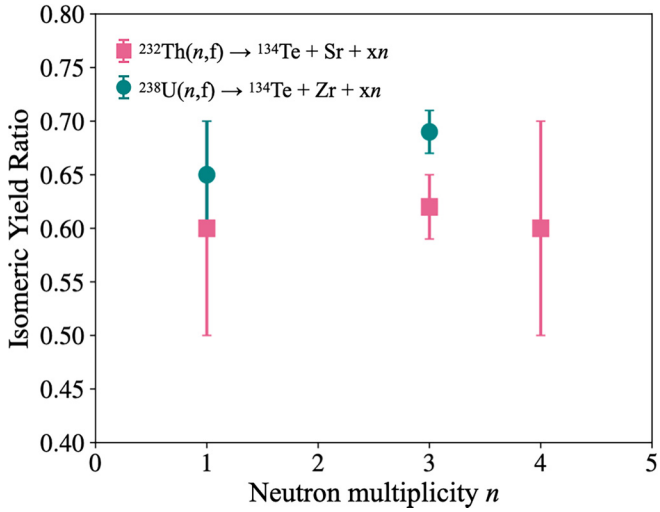

FIG. 7. Isomeric yield ratios of ^{134}Te from the reactions ^{238}U(n, f) and ^{232}Th(n, f) when a gate is placed on 2^+[^{134}Te] and a specified transition in the partner.

In Fig. 6, the IYR of ^{134}Te extracted from the different fissioning systems are observed to have a slope with mass number; however, this slope is at the limit of being statistically insignificant (0.004 ± 0.002).

Furthermore, Table I shows that increasing the average neutron energy from 1.9 to 3.4 MeV in the case of ^{238}U(n, f) does not yield a statistically significant change in the IYR.

From Fig. 7, the IYR of ^{134}Te appears to be unaffected by the number of prompt neutrons emitted. Note from Table I that for the reaction ^{238}U(n, f) → ^{134}Te + Zr + xn the gates used on the Zr partners were both on the transition from the first 4^+ state. In the case of ^{232}Th(n, f) → ^{134}Te + Sr + xn, different transition gates were used for the various Sr partners.

However, Fig. 8 shows contradicting results. The partner gating on the ^{238}U(n, f) → ^{134}Te + ^{102}Zr + 3n data set does not give an observed change with minimum J of ^{102}Zr. On the other hand, in ^{232}Th(n, f) → ^{134}Te + ^{96}Sr + 3n the IYR drops significantly when the gate is changed from 2^+[^{96}Sr] to 4^+[^{96}Sr]. This is discussed in Sec. VI A. Due to the different gates used, we only compare the trends between the different systems and not the absolute IYR value [i.e., the IYR obtained from ^{238}U(n, f) → ^{134}Te + ^{102}Zr + 3n will not be directly compared to ^{232}Th(n, f) → ^{134}Te + ^{96}Sr + 3n].

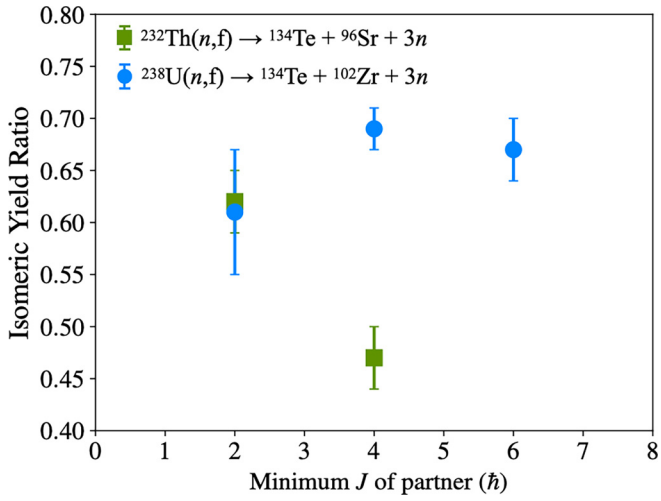

FIG. 8. Isomeric yield ratios of ^{134}Te from the reactions ^{238}U(n, f) and ^{232}Th(n, f) when a gate is placed on 2^+[^{134}Te] and the gate on the partner is changed.

V. DECAY SIMULATION: FREYA+TALYS

As stated in the introduction, IYR measurements are sensitive to the angular momentum of the primary fragment J_i. However, a model is needed to transform the measurement to a quantitative value of J_i. One such model that has been used previously is the one-parameter Madland-England model [31], but it was recently commented in Ref. [29] that this model is likely too simplistic to provide accurate values for J_i. We employed the Hauser-Feshbach decay code TALYS [32] to determine the angular momentum of the primary fragment from the measured IYR. The methodology was developed to interpret IYR experimental data from proton-induced fission isomeric yields at the IGISOL facility [22].

In order to deexcite fission fragments, TALYS requires their initial excitation energy E_x as well as J_i. This information was obtained from the fission simulation code FREYA [21,33] which yields the (correlated) (E_x, J_i) distributions of the primary Te fragments. This procedure is described in detail for the combination of the fission code GEF and TALYS in Ref. [22].

Version v.2.0.5 of FREYA was used, and the code was changed to allow the extraction of the angular momenta of the fission fragments. Furthermore, the reduction factor for the rigid-body value of the moment of inertia was changed from 0.3 to 0.5 for all fragments. All of the changes in the FREYA code can be viewed in Ref. [34].

FREYA was used to simulate ^{238}U(n, f) at the incoming neutron energy 1.9 MeV. Events resulting in a Te fragment with mass $A \geqslant 134$ were selected, and the E_x among these fragments were found to have an average value of 9 MeV with a dispersion of 4 MeV, while the J_i distribution had an average of $6\hbar$ with a dispersion of $3\hbar$.

To enable the possibility of varying the initial conditions of the nucleus in TALYS, the dependency between the distribution for E_x and J_i was parametrized separately for each A. The parametrization was based on the statistical model for deexcitation of the fragments, where the probability P of having a state of spin J is given by

$$P(J) \propto (2J+1)\exp\left(-\frac{(J+0.5)^2}{B^2}\right), \tag{4}$$

and B is an adjustable, E_x-dependent parameter related to the spin cutoff parameter σ ($B^2 = 2\sigma^2$), which governs the mean value and width of the spin probability distribution. Using Eq. (4), the value of B was transformed to the average angular momentum $\bar{J}_i$, as recent experimental results [2] provided this value instead of the B value. We would like to emphasize that the average angular momentum $\bar{J}_i$ is not directly comparable to the root-mean-square value J_{rms} [1], which is also

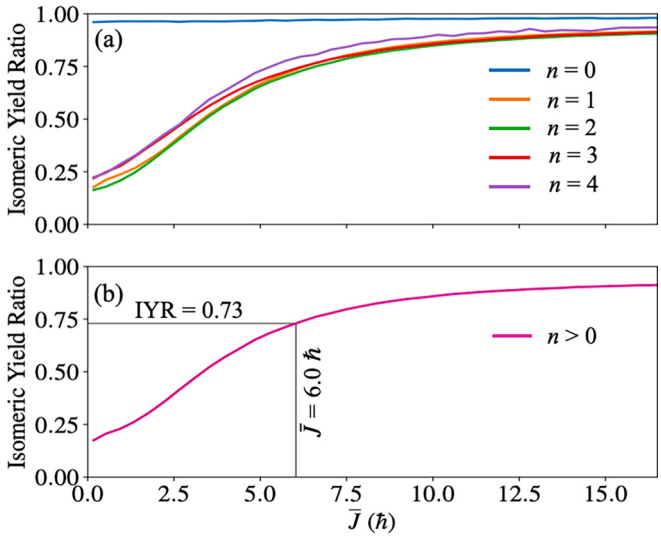

FIG. 9. The IYR of ^{134}Te as a function of the average initial angular momentum J_i of the primary fission fragment from the reaction ^{238}U(n, f) at $E_n = 1.9$ MeV. In (a), the IYR are only shown for the different neutron channels, and (b) shows the summed contribution for the $n > 0$ channels. In (b), the value of the measured IYR is marked along with $\bar{J}_i$ to which it corresponds.

sometimes used to describe an angular momentum distribution (see, e.g., Ref. [35]).

This parametrization describing the E_x and J_i of the initial nucleus was given to TALYS. New initial conditions for the fragments were sampled, and the resulting Te-precursors were de-excited. The amount of samples for each A reflects the initial distribution of fragment masses from FREYA. A minor modification was made in the TALYS code such that the decay was stopped once it reached one of the energy levels in Fig. 3. The calculated IYR could be determined by looking at the relative population of the different levels.

Through the parametrization, it is possible to calculate the IYR as a function of the average values for $\bar{J}_i$, and this is shown in Fig. 9.

When an initial Te fission fragment decays, there are several possible pathways that may result in the production of the isotope ^{134}Te. For example, the initial fragment could have been ^{136}Te before emitting two neutrons during deexcitation, resulting in the experiment detecting γ rays from ^{134}Te. Furthermore, the probabilities of populating different energy levels also vary with the average angular momentum of the initial nucleus $\bar{J}_i$. In Fig. 9(a), the IYRs of ^{134}Te are plotted as a function of $\bar{J}_i$ for the different neutron multiplicity channels, e.g., the $n = 1$ channel indicate that the initial nucleus created in fission was ^{135}Te.

As a general trend for the $n > 0$ channels, Fig. 9(a) shows that for a low $\bar{J}_i$ the corresponding IYR is low. The IYR then increases as a function of $\bar{J}_i$, until it saturates at high $\bar{J}_i$. The exception is the $n = 0$ channel where TALYS suggests that the IYR is close to 1 for all values of $\bar{J}_i$. As the isomeric state has an angular momentum of $6\hbar$, the probability of populating this state when starting with close to zero $\bar{J}_i$ ought to be very small, since it requires multiple γ-ray transitions "uphill" to higher spin states in regions of relatively lower level density. Therefore, the behavior of the $n = 0$ channel in the low spin range appears to be unphysical and we exclude it in the further calculations. The $n > 0$ channels show the expected behavior where the IYR increases with increased $\bar{J}_i$ of the initial Te fragment.

The resulting IYR in pink in Fig. 9(b) is calculated by summing all population contributions from the neutron channels $n > 0$.

TALYS is known to have a J cutoff at $J = 30$, which might create an artificial saturation effect at high angular momenta. However, we see from Fig. 9 that the saturation starts at much lower values for J, which points to a real saturation effect. The existence of an IYR saturation effect is supported by Ref. [9], where the isomer saturation effect was observed in CGMF simulations of four other fission fragments. This will be further discussed in Sec. VI B. For now we point out that Fig. 9(b) shows that a small change in measured IYR will lead to a corresponding change in $\bar{J}_i$.

The figure also illustrates that to reproduce the experimental double-gated IYR result of 0.73 following the reaction ^{238}U(n, f) at $\bar{E}_n = 1.9$ MeV, the initial average angular momentum must be $6.0\hbar$. This reproduced the $\bar{J}_i$ of the initial FREYA distribution.

VI. DISCUSSION

A. Measured IYRs

1. Interpretation of IYR

Table I shows that when using the gate 2^+[^{134}Te] & 4^+[^{134}Te] to extract the IYR of ^{134}Te produced in the ^{238}U(n, f) reaction, the IYR is 0.73 ± 0.01. The interpretation is that whenever ^{134}Te is populated in the 4^+ state, then there is a 73% chance that it is also populated in the 6^+ state. This measurement provides a benchmark for fragment decay codes when calculating the initial spin distribution of ^{134}Te. Compared to the double gate, a single gate on only 2^+[^{134}Te] is expected to give a lower IYR value. This is due to the inclusion of the direct feeding to the 2^+ state, as illustrated in Fig. 3. However, this single-gated IYR value will come with a significant uncertainty due to the higher level of background, and thus all the extracted IYRs are determined using double gates.

2. Changing fissioning system

When comparing the IYR of ^{134}Te from the gate 2^+[^{134}Te] & 4^+[^{134}Te] across all three fissioning systems, ^{238}U(n, f), ^{232}Th(n, f), and ^{252}Cf(sf), a linear regression fit of the IYR dependence on the mass number gives a slope of 0.004 ± 0.002. The slope is not sufficiently significant to allow a conclusion about a variation between the systems. This observation is therefore consistent with the findings of Ref. [2], even considering the higher sensitivity to small differences in J_i that IYR measurements might provide.

An independence in the observed IYR on the mass number of the fissioning system was also observed in the 2021 evaluation of the available IYR literature [29], and it was stated that within the uncertainties there was no dependency of the IYR

on the target nucleus for the four well-studied nuclei ^{128}Sb, ^{131}Te, ^{134}I, and ^{138}Cs. On the other hand, Ref. [19] observed changes in the IYR of Sn and Y isotopes between $^{\text{nat}}U(p,\text{f})$ and ^{232}Th(p,f), where the Sn isotopes had higher IYR values following $^{\text{nat}}U(p,\text{f})$, while the opposite occurred for the Y isotopes. This was attributed to potential variations in the scission deformations of the nuclei between the different systems.

The impact of fission-fragment deformation on IYRs has been observed several times. In Ref. [10], the IYRs were measured for a chain of Cd and I isotopes, and a positive correlation between the fragment's J_{i} and quadrupole moment was found. They also observed the impact of unpaired protons on the IYR, where the added angular momentum of the unpaired proton yields a higher IYR. This effect had previously been observed [36] and it was also commented that fragments close to spherical shells also have a lower J_{i}. The observation of the effect of unpaired protons also demonstrates the high degree of sensitivity to IYR measurements to the angular momentum of the fragment. Finally, Ref. [4] measured the IYR of ^{132}Sn as a function of the fragment's kinetic energy and found an increase in IYR with lower kinetic energy. Again, this supports the deformation-dependence of IYRs as less kinetic energy is attributed to more deformed scission shapes.

The evidence for the fragment deformation effect on IYR is thus quite substantial. Given that the determined IYRs for ^{134}Te in this work do not vary much (if at all) with the mass number of the fissioning system, this indicates that the scission shapes may be similar when the fragment is produced in ^{238}U(n,f), ^{232}Th(n,f), and ^{252}Cf(sf).

3. Changing excitation energy of the CN

The IYR measured following the neutron-induced fission of ^{238}U at either $\bar{E}_n = 1.9$ or 3.4 MeV is the same within the uncertainties. Though adding ≈1.4 MeV to the fissioning system might not seem like a significant change, this difference is similar to the energy gap between thermal neutron induced and fast neutron induced fission. The difference in γ emission between thermal and fast fission has been deemed an important point to measure, due to potential increased γ-ray heating in fast reactors [13]. Our observation of no change in the IYR over this energy range conforms with the comparison in Ref. [29] between existing IYR measurement at thermal and fast energies, IYRs measured following bremsstrahlung-induced fission [37] as well as with previous measurements showing that the fission γ-ray multiplicity does not change significantly with small changes in the excitation energy of the compound nucleus (CN) [38,39].

If the excitation energy range is significantly increased, however, the literature indicates that this might affect the IYRs. Reference [40] studied the IYRs of ^{121}Cd and ^{135}Xe from ^{232}Th(p,f) for proton energies from 13 to 26 MeV, and found a small increase in the IYR for increasing proton energy, which also conforms with older results [14,41]. This is not necessarily in conflict with the results above, due to the significantly larger gap in E_{x} investigated in those works. It should also be noted that over such large changes in the E_{x}, multichance fission will lead to changes in the mass of the nucleus that undergoes fission.

4. Neutron multiplicity gating

The partner gating was used to control the emitted neutron multiplicity, and the IYRs extracted from the ^{238}U$(n,\text{f}) \rightarrow {}^{134}\text{Te} + {}^{102}\text{Zr} + 3n$ and $^{134}\text{Te} + {}^{104}\text{Zr} + 1n$ systems are compared. From the method itself one cannot determine how many neutrons were emitted from the ^{134}Te precursor compared to the Zr partner; however, this is information available from the FREYA simulation. We find from FREYA simulations that the ^{134}Te precursor emits about 0.7 neutrons more on average when the neutron multiplicity of the event increases from $1n$ to $3n$, and thus the difference in IYRs extracted for ^{134}Te reflects the impact of about one extra neutron emitted from the initial nucleus.

There are two ways that the neutron could impact the angular momentum J and thus IYR of the fragment. First, Ref. [28] suggested that neutrons might carry more angular momentum from the fission fragments than is widely thought, and that they could reduce J with a value of more than $1\hbar$ on average, i.e., $\Delta J = 1.34 \pm 1.93\,\hbar$ for ^{238}U(n,f). An increase in neutron multiplicity might thus remove more angular momentum prior to γ emission, resulting in a decrease in the IYR.

Furthermore, the number of neutrons emitted by a fragment reflects the initial excitation energy at which the fragment was produced, as neutrons are largely emitted prior to γ rays in the deexcitation process. More neutrons emitted therefore indicates a higher excitation energy of the primary fragment after scission. Specifically for the case studied here, the neutron separation energy of the $1n$ precursor nucleus ^{135}Te is ≈3.3 MeV [42]. As some suggestions for angular momentum generation mechanisms are rooted in the available excitation energy of the fragments [2,35,43], IYRs of the neutron-gated systems therefore provide valuable information.

The IYRs extracted for the $^{134}\text{Te} + {}^{102}\text{Zr} + 3n$ system are within a 2σ interval of the value from $^{134}\text{Te} + {}^{104}\text{Zr} + 1n$, revealing that, within the sensitivity, the angular momentum of ^{134}Te is independent of the number of prompt neutrons emitted by the fissioning system. This implies that the neutrons do not carry a very large amount of angular momentum, and that the difference in the excitation energy at which the ^{134}Te precursor is produced does not have any significant impact. The latter is thus another confirmation of the E_{x} independence of the IYR of ^{134}Te, which spans a larger excitation energy difference (2.3 MeV) than the 1.4 MeV change in CN energy between neutron-induced fission at $\bar{E}_n = 1.9$ vs 3.4 MeV.

The independence of ^{134}Te on neutron multiplicity is also seen for ^{232}Th(n,f), though the uncertainties on these measurements are larger due to the difficulty of finding appropriate transitions for the partner gate.

Our finding that the IYRs do not depend on the neutron multiplicity indicates that neutrons do not remove significant amounts of angular momentum ΔJ. However, ΔJ is only constrained within the uncertainties on the measurements, and thus might still be consistent with the suggested ΔJ in Ref. [28]. In the future, experiments with better statistics will be able to investigate more precisely the angular momentum removal by neutron evaporation.

5. Partner J gating

Finally, the ^{134}Te + ^{102}Zr +3n system was considered, where gates are placed progressively higher in the level scheme of ^{102}Zr. Figure 8 shows that there is no significant change in the IYR of ^{134}Te when demanding higher average minimum J in the partner. One reason for this could be that the gates are not selective enough such that there is little change in the J_i distribution of ^{102}Zr with a 2^+ vs 6^+ gate. This would especially be a challenge if the average angular momentum of the partner was sufficiently high. However, Ref. [2] lists that the average angular momentum following ^{238}U(n, f) for ^{102}Zr is about 6$\hbar$, meaning that roughly half of the distribution is expected to be omitted when placing a gate on the 6^+ transition. Thus the independence observed in the IYR supports the findings presented in Ref. [2] that the angular momenta of the two fission fragments are uncorrelated in magnitude.

The same procedure of increasing the partner J was conducted for the ^{134}Te + ^{96}Sr +3n system, which emerged from the ^{232}Th(n, f) reaction. Contrary to the observation above, the gates on the ^{96}Sr 2^+ state versus 4^+ state yield statistically significant differences in the IYR. Whether this is merely a statistical deviation or a true trend caused by structure effects will be investigated in upcoming experiments.

B. TALYS simulations

The average angular momentum of the ^{134}Te precursor was determined from the FREYA+TALYS simulations in Fig. 9(b) to be 6.0 $\hbar$. This, as commented above, reproduces the original average of 6$\hbar$ that FREYA gave, indicating that the original J distribution from FREYA provides a good representation of the experimental angular momentum distribution of Te fragments.

Reference [44] used FIFRELIN to extract the average angular momentum as a function of the fission fragment mass for ^{252}Cf(sf). Their value for J_i changes rapidly in the $A = 134$ region and is between 6-9$\hbar$. This is in agreement with our results.

Furthermore, our value of $\bar{J}_i$ deviates significantly from the CGMF simulations presented in Ref. [28] Fig. 2(b), where the initial angular momentum prior to statistical neutron and γ-ray emission was about 9.5$\hbar$. A possible reason for this deviation might be the assumptions regarding angular momentum removal by neutrons, which in Ref. [28] is found to be significant. It is shown that it is possible to reproduce the angular momentum sawtooth in Ref. [2] even if one assumes that the neutrons carry more than 1$\hbar$ of angular momentum on average. As discussed in Sec. VI A, we do not see a change in J with increased neutron multiplicity within the sensitivity of the method, but the precise amount is yet to be determined experimentally. The value for J poststatistical neutron and gamma emission in Ref. [28] fits well with the FREYA+TALYS values for prestatistical emission.

Furthermore, the value of $\bar{J}_i$ of ^{134}Te presented in Ref. [2] was $4.26 \pm 0.17\,\hbar$. This deviates from the value presented here. However, this may be caused by an overestimate of the direct feeding of the 2^+ due to the presence of the isomer.

Saturation effects

An important aspect of information revealed by the TALYS simulations is the sensitivity of the IYR measurement to changes in J_i. As seen in Fig. 9, the feeding of the isomer in ^{134}Te changes as a function of the angular momentum of the primary fragment. In a range of $\bar{J}_i$, the IYR changes rapidly with small changes in $\bar{J}_i$ and is thus a highly sensitive probe of small differences between systems. However, if the J of the isomeric state is too low, the feeding of the isomer saturates. As it is no longer sensitive to $\bar{J}_i$ after the IYR feeding has saturated, it is not a good metric for determining the J_i. On the other hand, if the J of the isomeric state is too high, it will not be populated in fission, and thus the IYR carry little information on the initial angular momentum of the fragment. An isomeric state is thus only a good tool for investigating $\bar{J}_i$ as long as the spin of the isomeric state is comparable to the $\bar{J}_i$. The feeding saturation is also dependent on where in the level scheme this state is found; isomers at low excitation energies saturate more quickly than high-lying states.

When investigating differences between fissioning systems and reactions, saturation of the isomer feeding could result in unchanged values for the IYR. This is a potential explanation for the observation that some fragments have IYRs that change with differences in the fissioning system [19], while others do not [29]. However, in the current study of ^{134}Te we observe from the TALYS simulations that the isomer is not expected to be saturated for this value of the IYR. In fact, it is still highly sensitive to changes in the J_i, where a change of 1% in the IYR results in a change of 2.1% in $\bar{J}_i$.

Though a saturation of the isomer feeding leaves the IYR insensitive to further changes in the angular momentum of the fragment, this still provides a benchmark for fission codes to determine the E_x and J_i of the primary fragment.

In this work we have pointed out several possible ways that the measured IYR could not be reflective of the initial angular momentum distribution in the fission fragment. In addition to the isomer saturation effect, we have also discussed the possibility of contamination from β decay, as well as the limitations in the model used to transform between the IYR and $\bar{J}_i$. These effects, in addition to possible systematic differences in experiments, might have impacted the establishment of the angular momentum sawtooth dependence on the mass of the fission fragment [2,3,45], as one study of IYRs saw the structure [35] while another did not [16].

VII. CONCLUSION AND OUTLOOK

In this paper, we have studied the impact on the IYR of changing the fissioning system, the CN excitation energy, the minimum J of the binary partner, and the number of neutrons emitted from the fissioning system.

We have presented a new method for extracting IYRs, where the arrival time of discrete γ rays is used to decouple the prompt and isomeric decays of a nucleus. The method was applied to the fission fragment ^{134}Te, and IYRs of the 6^+ isomeric state were extracted from the three different systems ^{238}U(n, f) at $\bar{E}_n =$ 1.9 MeV, ^{232}Th(n, f) at $\bar{E}_n =$ 2.0 MeV, and ^{252}Cf(sf), as well as at a higher CN excitation energy for the ^{238}U(n, f) case ($\bar{E}_n =$ 3.4 MeV). The change in IYR

with mass of the fissioning system shows a slight increase, but only has a 2σ statistical significance. Previous measurements have both seen [19] and not seen [29] variations with CN mass. Potential changes in the IYR with different fissioning systems might originate from changing scission shape. More investigations are needed to clarify the impact on specific isotopes.

The IYRs extracted for different CN E_x are the same within the uncertainties, conforming with the previous observations that small changes in E_x does not change the IYR [29].

By using γ-ray gates to constrain the properties of the partner fragment that emerges with ^{134}Te, the impact on the IYR of neutron multiplicity and increase in partner J was investigated. An increased neutron multiplicity did not change the ^{134}Te IYR, which indicates that the neutrons carry small amounts of angular momentum ΔJ. Future experiments will be able to constrain ΔJ by achieving smaller statistical uncertainties. The impact of the IYR on partner J yielded contradicting results for the cases $^{238}\mathrm{U}(n,\mathrm{f}) \rightarrow {}^{134}\mathrm{Te} + {}^{102}\mathrm{Zr} + 3n$ and $^{232}\mathrm{Th}(n,\mathrm{f}) \rightarrow {}^{134}\mathrm{Te} + {}^{96}\mathrm{Sr} + 3n$, and further investigations are needed.

Simulations conducted by combining FREYA and TALYS were used to determine the average angular momentum magnitude of ^{134}Te following $^{238}\mathrm{U}(n,\mathrm{f})$, which was found to be $6\hbar$. The effect of isomer feeding saturation was also discussed, and we showed that there is a limited range, where the IYR of a specific isomer is a good measure of the angular momentum of the initial nucleus.

In the future, new experiments could provide higher-statistics data sets that would allow the expansion of this method to measurements of lower-yield isomers. More measurements in the light-fragment region would be especially interesting, as it has been pointed out that IYR measurements have mainly focused on the heavy fragment [29]. Partner gating may also be pursued to determine more accurately the amount of angular momentum carried off by neutrons from fission fragments.

ACKNOWLEDGMENTS

We thank the staff of the ALTO facility of the IJC Laboratory, Orsay, for providing the ^{7}Li primary beams, and we thank the Gammapool international consortium for the loan of the germanium clover detectors used to construct the ν-Ball spectrometer. The authors thank L. Gaudefroy for the loan of the fission chamber for the ^{252}Cf(sf) experiment. D.G. acknowledges funding from the Research Council of Norway (Norges Forskningsråd) Grant No. 263030, and thanks S. Marin for discussions. This work was supported by the IN2P3/CNRS, France, the STFC UK Nuclear Data Network, the STFC (Grants No. ST/L005743/1 and No. ST/P005314) (P.H.R.), and the Marion Redfearn Trust (RCL). P.H.R., M.B., A.Boso and P.I. acknowledge support from the UK Department of Business, Energy and Industrial Strategy (BEIS) via the National Measurement System. P.K., P.-A.S., and J.W. acknowledge the support from BMBF under Grant No. NuSTAR.DA 05P15RDFN1. P.-A.S. also acknowledges the support from by the Romanian Ministry of Research, Innovation and Digitalization under Contract No. PN 23.21.01.06. Funding from the HORIZON2020 program of the European Commission is acknowledged for transnational access to the ALTO facility under the Integrated Infrastructure Initiative, European Nuclear Science and Applications Research 2 (ENSAR2), Grant Agreement No. 654002. A.B., R.-B.G., and N.W. acknowledge support by the German Research Foundation (DFG Grant No. BL 1513/1-1). L.F., V.V., J.B., and V.S.-T. acknowledge funding from the Spanish MINECO via FPA2015-65035-P and RTI2018-098868-B-I00. A.A. acknowledges funding from the Spanish MINECO via FPA2017-83946-C2-1-P and Ministerio de Ciencia e Innovacion Grant No. PID2019-104714GB-C21. B.F. acknowledges funding from the Polish National Science Centre under Contracts No. 2014/14/M/ST2/00738 and No. 2013/08/M/ST2/00257. M.P.S. acknowledges funding from the Polish National Science Centre under Contracts No. UMO-2019/33/N/ST2/03023 and No. UMO-2020/36/T/ST2/00547, and A.K., K.M., and E.A. acknowledge funding under Contract No. UMO-2015/18/E/ST2/00217. S.L., G.B., C.P., S.Z., L.W.I, A.G., and S.B. acknowledge funding from the Italian Istituto Nazionale di Fisica Nucleare (INFN). L.I. acknowledges funding from the Polish National Science Centre, Poland, under research Project No. 2020/39/D/ST2/03510. This work was partially funded by the Polish National Science Center under Grant No. 2020/39/B/ST2/02346.

[1] J. B. Wilhelmy, E. Cheifetz, R. C. Zared, S. G. Thompson, H. R. Bowman, and O. Rasmussen, Angular momentum of primary products formed in the spontaneous fission of ^{252}Cf, Phys. Rev. C **5**, 2041 (1972).

[2] J. N. Wilson *et al.*, Angular momentum generation in nuclear fission, Nature (London) **590**, 566 (2021).

[3] M. Travar *et al.*, Experimental information on mass- and TKE-dependence of the prompt fission γ-ray multiplicity, Phys. Lett. B **817**, 136293 (2021).

[4] A. Chebboubi *et al.*, Kinetic energy dependence of fission fragment isomeric ratios for spherical nuclei ^{132}Sn, Phys. Lett. B **775**, 190 (2017).

[5] R. Vogt and J. Randrup, Angular momentum effects in fission, Phys. Rev. C **103**, 014610 (2021).

[6] A. Bulgac, I. Abdurrahman, S. Jin, K. Godbey, N. Schunck, and I. Stetcu, Fission fragment intrinsic spins and their correlations, Phys. Rev. Lett. **126**, 142502 (2021).

[7] P. Marevic, N. Schunck, J. Randrup, and R. Vogt, Angular momentum of fission fragments from microscopic theory, Phys. Rev. C **104**, L021601 (2021).

[8] J. R. Huizenga and R. Vandenbosch, Interpretation of isomeric cross-section ratios for (n,γ) and (γ,n) reactions, Phys. Rev. **120**, 1305 (1960).

[9] I. Stetcu, P. Talou, T. Kawano, and M. Jandel, Isomer production ratios and the angular momentum distribution of fission fragments, Phys. Rev. C **88**, 044603 (2013).

[10] V. Rakopoulos *et al.*, Isomeric fission yield ratios for odd-mass Cd and In isotopes using the phase-imaging

ion-cyclotron-resonance technique, Phys. Rev. C **99**, 014617 (2019).
[11] V. Guadilla *et al.*, Large impact of the decay of niobium isomers on the reactor $\bar{\nu}_e$ summation calculations, Phys. Rev. Lett. **122**, 042502 (2019).
[12] M. Estienne *et al.*, Updated summation model: An improved agreement with the Daya Bay antineutrino fluxes, Phys. Rev. Lett. **123**, 022502 (2019).
[13] G. Rimpault, D. Bernard, D. Blanchet, C. Vaglio-Gaudard, S. Ravaux, and A. Santamarina, Needs of accurate prompt and delayed γ-spectrum and multiplicity for nuclear reactor designs, Phys. Procedia **31**, 3 (2012).
[14] H. G. Hicks and R. S. Gilbert, Radiochemical studies of the high-energy fission process, Phys. Rev. **100**, 1286 (1955).
[15] R. A. Sharp and A. C. Pappas, ^{115}Cd isomer yield ratios from deuteron fission of ^{238}U and from the ^{118}Sn$(d, \alpha p)$, ^{118}Sn(n, α), ^{115}In$(d, 2p)$, ^{115}In(n, p) and ^{114}Cd(d, p) reactions from 10 to 25 MeV, J. Inorg. Nucl. Chem. **10**, 173 (1959).
[16] H. Naik, S. P. Dange, and R. J. Singh, Angular momentum of fission fragments in low energy fission of actinides, Phys. Rev. C **71**, 014304 (2005).
[17] T. Datta, S. P. Dange, S. K. Das, S. Prakash, and M. V. Ramaniah, Atomic nuclei influence of fission fragment nuclear structure on scission configuration in ^{252}Cf (S.F.), Z. Phys. A **324**, 81 (1986).
[18] R. Grzywacz *et al.*, Identification of μs-isomers produced in the fragmentation of a ^{112}Sn beam, Phys. Lett. B **355**, 439 (1995).
[19] V. Rakopoulos *et al.*, First isomeric yield ratio measurements by direct ion counting and implications for the angular momentum of the primary fission fragments, Phys. Rev. C **98**, 024612 (2018).
[20] A. A. Sonzogni, Nuclear data sheets for $A = 134$, Nucl. Data Sheets **103**, 1 (2004).
[21] J. Randrup and R. Vogt, Calculation of fission observables through event-by-event simulation, Phys. Rev. C **80**, 024601 (2009).
[22] A. Al-Adili, V. Rakopoulos, and A. Solders, Extraction of angular momenta from isomeric yield ratios employing TALYS to de-excite primary fission fragments, Eur. Phys. J. A **55**, 61 (2019).
[23] M. Lebois, N. Jovančević, J. N. Wilson, D. Thisse, R. Canavan, and M. Rudigier, The ν-ball campaign at ALTO, Acta Phys. Pol. B **50**, 425 (2019).
[24] M. Lebois, N. Jovančević, D. Thisse, R. Canavan, D. Étasse, M. Rudigier, and J. N. Wilson, The ν-ball γ-spectrometer, Nucl. Instrum. Methods Phys. Res. Sect. A **960**, 163580 (2020).
[25] L. Gaudefroy, S. Péru, N. Arnal, J. Aupiais, J.-P. Delaroche, M. Girod, and J. Libert, Impact of Coriolis mixing on a two-quasi-neutron isomer in ^{164}Gd$_{100}$ and other $N = 100$ isotones, Phys. Rev. C **97**, 064317 (2018).
[26] M. Lebois, J. N. Wilson, P. Halipré, B. Leniau, I. Matea, A. Oberstedt, S. Oberstedt, and D. Verney, Development of a kinematically focused neutron source with the $p(^7\text{Li}, n)^7$Be inverse reaction, Nucl. Instrum. Methods Phys. Res. Sect. A **735**, 145 (2014).
[27] D. Etasse, B. Carniol, C. Fontbonne, J.-M. Fontbonne, J. Harang, J. Hommet, H. Plard, J. Poincheval, T. Chaventré, and D. Cussol, Fast Acquisition System for nuclEar Research (FASTER), https://faster.in2p3.fr.
[28] I. Stetcu, A. E. Lovell, P. Talou, T. Kawano, S. Marin, S. A. Pozzi, and A. Bulgac, Angular momentum removal by neutron and γ-ray emissions during fission fragment decays, Phys. Rev. Lett. **127**, 222502 (2021).
[29] C. J. Sears, A. Mattera, E. A. McCutchan, A. A. Sonzogni, D. A. Brown, and D. Potemkin, Compilation and evaluation of isomeric fission yield ratios, Nucl. Data Sheets **173**, 118 (2021).
[30] Y. Abdelrahman, J. L. Durell, W. Gelletly, W. R. Phillips, I. Ahmad, R. Holzmann, R. V. F. Janssens, T. L. Khoo, W. C. Ma, and M. W. Drigert, Average spins of primary fission fragments, Phys. Lett. B **199**, 504 (1987).
[31] D. G. Madland and T. R. England, The influence of isomeric states on independent fission product yields, Nucl. Sci. Eng. **64**, 859 (1977).
[32] A. Koning, S. Hilaire, and S. Goriely, TALYS: modeling of nuclear reactions, Eur. Phys. J. A **59**, 131 (2023).
[33] J. Randrup and R. Vogt, Refined treatment of angular momentum in the event-by-event fission model FREYA, Phys. Rev. C **89**, 044601 (2014).
[34] J. Randrup, R. Vogt, J. M. Verbeke, and D. Gjestvang, FREYA v.2.0.5 - changes for ^{134}Te IYR article, GitHub, https://github.com/dortheg/fission_v2.0.5/tree/clean_FREYA, 2022.
[35] M. Tanikawa, H. Kudo, H. Sunaoshi, M. Wada, T. Shinozuka, and M. Fujioka, Isomeric yield ratios of fission products in the system of 24 MeV proton-induced fission of ^{238}U, Z. Phys. A **347**, 53 (1993).
[36] H. Naik, S. Dange, R. Singh, and T. Datta, Systematics of fragment angular momentum in low-energy fission of actinides, Nucl. Phys. A **587**, 273 (1995).
[37] H. Thierens, B. Proot, D. De Frenne, and E. Jacobs, Independent isomeric yield ratio of ^{123}I in the photofission of ^{235}U and ^{238}U, Phys. Rev. C **25**, 1546 (1982).
[38] J.-M. Laborie, R. Billnert, G. Bélier, A. Oberstedt, S. Oberstedt, and J. Taieb, First experimental prompt γ-ray spectra in fast-neutron-induced fission of ^{238}U, Phys. Rev. C **98**, 054604 (2018).
[39] D. Gjestvang *et al.*, Excitation energy dependence of prompt fission γ-ray emission from ^{241}Pu*, Phys. Rev. C **103**, 034609 (2021).
[40] S. Goto, D. Kaji, H. Kudo, M. Fujita, T. Shinozuka, and M. Fujioka, Isomeric yield ratios of fission products in proton-induced fission of ^{232}Th, J. Radioanal. Nucl. Chem. **239**, 109 (1999).
[41] D. G. Sarantites, G. E. Gordon, and C. D. Coryell, Ratios of independent yields of the isomers $^{131-131m}$Te and $^{133-133m}$Te in fission, Phys. Rev. **138**, B353 (1965).
[42] B. Singh, A. A. Rodionov, and Y. L. Khazov, Nuclear data sheets for $A = 135$, Nucl. Data Sheets **109**, 517 (2008).
[43] T. Døssing, S. Åberg, M. Albertsson, B. Carlsson, P. Möller, and J. Randrup, Angular momentum in fission fragments, Phys. Rev. C (to be published).
[44] V. Piau *et al.*, Neutron and gamma multiplicities calculated in the consistent framework of the Hauser-Feshbach Monte Carlo code FIFRELIN, Phys. Lett. B **837**, 137648 (2023).
[45] P. Armbruster, H. Labus, and K. Reichelt, Investigation on the primary spins of the ^{235}U fission fragments, Z. Naturforsch. A **26**, 512 (1971).